ADVANCES IN ATMOSPHERIC SCIENCES, VOL. 26, NO. 2, 2009, 312–318

Model Analysis of Seasonal Variations in Tropospheric Ozone and Carbon Monoxide over East Asia

GAO Lijie[1,3] (高丽洁), ZHANG Meigen[*1] (张美根), and HAN Zhiwei[2] (韩志伟)

[1] *State Key Laboratory of Atmospheric Boundary Layer Physics and Atmospheric Chemistry, Institute of Atmospheric Physics, Chinese Academy of Sciences, Beijing* 100029

[2] *Key Laboratory of Regional Climate-Environment Research for Temperate East Asia, Institute of Atmospheric Physics, Chinese Academy of Sciences, Beijing* 100029

[3] *Graduate University of Chinese Academy of Sciences, Beijing* 100049

(Received 1 November 2007; revised 17 February 2008)

ABSTRACT

Temporal-spatial variations in tropospheric ozone concentrations over East Asia in the period from 1 January 2000 to 31 December 2004 were simulated by using the Models-3 Community Multi-scale Air Quality (CMAQ) modeling system with meteorological fields calculated by the Regional Atmospheric Modeling System (RAMS). The simulated concentrations of ozone and carbon monoxide were compared with ground level observations at two remote sites, Ryori (39.03°N, 141.82°E) and Yonagunijima (24.47°N, 123.02°E). The comparison shows that the model reproduces their seasonal variation patterns reasonably well, and simulated ozone levels are generally in good agreement with the observed ones, but carbon monoxide concentrations are underestimated. Analysis of horizontal distributions of monthly averaged ozone mixing ratios in the surface layer indicates that ozone concentrations have noticeable differences among the four seasons; they are generally higher in the spring and summer while lower in the winter, reflecting the seasonal variation of solar intensity and photochemical activity and the fact that the monsoons over East Asia are playing an important role in ozone distributions.

Key words: tropospheric ozone, East Asia, seasonal variations, long-range transport

Citation: Gao, L. J., M. G. Zhang, and Z. W. Han, 2009: Model analysis of seasonal variations in tropospheric ozone and carbon monoxide over East Asia. *Adv. Atmos. Sci.*, **26**(2), 312–318, doi: 10.1007/s00376-009-0312-9.

1. Introduction

Resent researches suggest that tropospheric ozone concentrations have increased in the lower troposphere over East Asia in recent decades and the rate of increase is larger than in other areas of the northern mid-latitudes (Akimoto et al., 1994; Oltmans et al., 1998; Lee et al., 1998). Simulations also suggest that man-made emissions at low northern latitudes, in particular in southern and eastern Asia, will become a very strong tropospheric ozone source in the future (Lelieveld and Dentener, 2000).

Seasonal variations in tropospheric ozone have been documented in many observational studies in the northern hemisphere. These studies found that ozone exhibits a spring maximum and a summer minimum at many remote sites in East Asia (Monks, 2000; Pochanart et al., 2002). While measurements at the Waliguan station (36°17′N, 100°54′E), located in a remote region of the Tibetan Plateau and at a height of 3810 m above sea level, show different characteristics with a maximum in summer and a minimum in winter (Tang et al., 1995). By using a regional air pollution modeling system (RAPMS), Zhu et al. (2004) attributed this feature to the evolution of the East Asian monsoon system in combination with photochemical production. As to the spring maximum of many observations on the East Asian Pacific rim, some

*Corresponding author: ZHANG Meigen, mgzhang@mail.iap.ac.cn

research suggested that the contribution of stratospheric ozone compared to surface ozone levels is quite limited (Zhang et al., 2004) because the incursion of stratospheric ozone into the troposphere reaches its maximum in winter at mid to high latitudes (Holton, 1990) and is difficult to be transported to the surface layer. A global model study by Mauzerall et al. (2000) showed that net ozone production from spring through autumn has a maximum in central East Asia resulting from the strong emission and transport of anthropogenic ozone precursors.

In this study the Models-3 Community Multi-scale Air Quality (CMAQ) modeling system (Byun and Ching, 1999) coupled with the Regional Atmospheric Modeling System (RAMS) (Pielke et al., 1992) was applied to East Asia to simulate the transport and transformation of tropospheric ozone in the period from 1 January 2000 to 31 December 2004, and then to explore the major processes determining its temporal-spatial distributions in the surface layer. To our knowledge, there are few papers that have reported simulations of tropospheric ozone in a period over one year using a regional chemical transport model.

2. Model Description

The model used in this study has two major components: CMAQ and RAMS. CMAQ is an Eulerian-type model for concurrently simulating all atmospheric and land processes that affect the transport, transformation, and deposition of air pollutants and their precursors on both regional and urban scales (Byun and Ching, 1999). RAMS is a highly versatile numerical code for simulating and forecasting meteorological phenomena. In this study RAMS is used to produce regional scale meteorological fields including boundary layer turbulence, cloud cover and precipitation necessary for the CMAQ inputs. CMAQ coupled with RAMS has recently been successfully applied to East Asia to simulate tropospheric ozone and sulfur dioxide (Zhang et al., 2002, 2004).

CMAQ can be configured with various degrees of complexity and choices of optional science modules. In this study, the chemical mechanism used in CMAQ is SAPRC99 (Carter, 2000) with modification to include dynamics and chemistry of aerosols and cloud chemistry. Compared with other photochemical mechanisms, SAPRC99 includes more detailed organic chemistry and explicit organic peroxy radicals. It provides better representation of peroxides for low NO_x and more complete organic intermediates. All these are important for the ozone simulations.

The study domain is 6240×5440 km^2 for CMAQ on a rotated polar-stereographic map projection centered at (25°N, 115°E) with 80×80 km^2 grid resolution covering Japan, Korea Peninsula, Southeast Asia and most of China. This region has dramatic variations in topography and land type, with mixtures of industrial and urban centers and rural agricultural regions. There are 14 vertical σ_z layers unequally spaced from the ground to ~23 km, with about half of the layers concentrated in the lowest 2 km of the atmosphere in order to resolve the planetary boundary layer.

For RAMS, the modeling domain is 8000×5600 km^2 with the same projection center as CMAQ. There are 23 vertical layers spaced from the ground to ~23 km with the lowest 7 layers being the same as those in CMAQ. The three-dimensional meteorological fields for the RAMS inputs are obtained from the European Center for Medium-range Weather Forecasts (ECMWF) $1°\times1°$ reanalysis data sets of 6-hour intervals. Sea surface temperatures (SST) for RAMS are based on weekly mean values.

For the CMAQ inputs, anthropogenic emissions were mainly obtained from the emission inventory of $1°\times1°$ prepared to support TRACE-P (TRAnsport and Chemical Evolution over the Pacific) and ACE-Asia (Asian Pacific regional Aerosol Characterization Experiment), while the emissions from biomass burning were adopted from the Global Emissions Inventory Activity (GEIA/POET) (Oliver et al., 2003). The emission rates are monthly averages and have no annual variations during the simulation period.

Initial and boundary conditions of chemical species in CMAQ were chosen to reflect the East Asian situation. Recent measurements were used whenever possible. To evaluate the impact of the anthropogenic emissions on the distributions of trace gases and aerosols, the initial and boundary conditions were generally chosen at the lower end of their observed range so as to allow the emissions and chemical reactions to bring them closer to their actual values during the initialization period (Zhang et al., 2003).

3. Results and discussion

3.1 *Model evaluation*

The transport and photochemical production of tropospheric ozone in the period from 1 January 2000 to 31 December 2004 are simulated. For evaluating the model's performance, model results are compared with observed surface concentrations of ozone and carbon monoxide at two remote sites, Ryori and Yonagunijima, in Japan. The Ryori site is located halfway up a mountainous cape in central Japan facing the Pacific Ocean at 39.03°N, 141.82°E and 260 m above sea level (asl). Yonagunijima is an isolated island, located about 100 km east of Taiwan. The sampling site

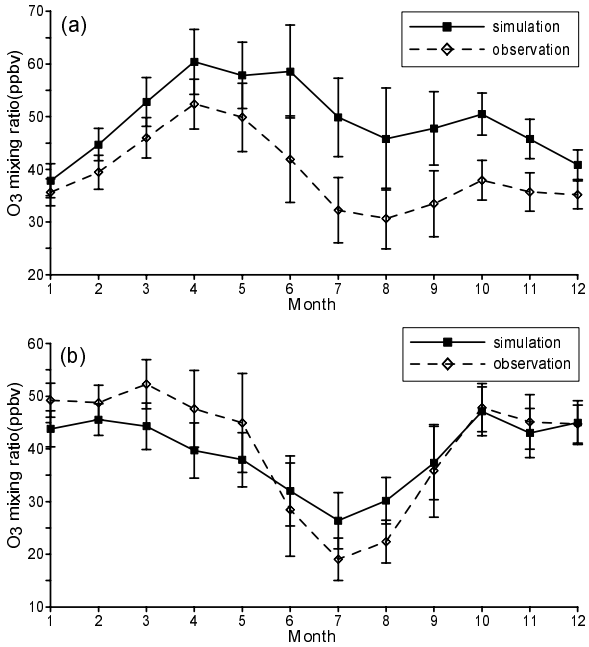

Fig. 1. Seasonal variations of simulated monthly mean ozone mixing ratios (solid lines, ppbv) at the lowest model layer (∼75 m above the ground) and observed ground-level monthly mean ozone concentrations (dashed lines, ppbv) at (a) Ryori and (b) Yonagunijima over the period 2000–2004. Error bars represent one standard deviation of the hourly mean ozone mixing ratios.

(24.47°N, 123.02°E and 30 m asl) is located near the northern coast of the island. Local emissions at the both sites are negligible.

Figure 1 shows the seasonal variations of monthly averaged surface ozone mixing ratios in the period from 1 January 2000 to 31 December 2004 measured at Ryori (Fig. 1a) and Yonagunijima (Fig. 1b). Also shown are model results at the lowest model layer approximately 75 m above the ground. Error bars represent one standard deviation of the hourly mean ozone mixing ratios. At Yonagunijima, the observed seasonal ozone variation shows a minimum in summer and high values in winter, which is a typical pattern of many remote locations both in the Northern and Southern Hemispheres (Monks, 2000). The simulation can successfully capture this pattern with a slight overestimation in winter and a slight underestimation in spring. The seasonal variations in ozone concentrations depend on multiple factors, such as the proximity to large source areas of ozone precursors, geographical location and meteorological conditions, so the above two different kinds of ozone seasonal cycle patterns may reflect two different ozone production modes. Yonagunijima is an isolated island and its location is below 30°N; its ozone concentrations result primarily from the long-range transport of air masses under the Asian monsoon regime (Pochanart et al., 2002). Good agreement between observations and simulations at this site indicates that the model can capture the general features of ozone variations in a clean marine boundary layer.

By contrast, the observed surface ozone seasonal variations at Ryori exhibit a clear spring maximum characteristic of the surface ozone seasonal cycle in a clean and remote atmosphere across the mid-latitudes in the Northern Hemisphere.

Figure 1a shows that both simulated and observed ozone concentrations are high in spring and low in summer, while the model tends to overestimate over the year as a whole. Ryori is located north of 30°N, belonging to the East Asia monsoon area, which can be affected by continental outflow except in summer. Analysis indicates that the overestimation might be explained by a relatively high contribution of continental outflow in the simulation.

Table 1 presents the statistical summaries of the comparison of modeled and observed hourly averaged concentrations of O_3 at Yonagunijima and Ryori. Table 2 is the same but for CO. From the tables we can see that the model values are generally in good agreement with their observed ones. For O_3, their correlation coefficients at Ryori for 2000, 2001, 2002, 2003 and 2004 are 0.77, 0.61, 0.72, 0.60 and 0.69, respectively. Correlation coefficients at Yonagunijima are even higher, reaching 0.87, 0.91, 0.82, 0.84, and 0.95, respectively. From the table, we also find that the annual average ozone concentrations are similar during these 5 years, and the seasonal variation patterns are quite similar.

Surface CO mixing ratios are also compared with observations at Ryori (Fig. 2a) and Yonagunijima (Fig. 2b). From Fig. 2 we can see that the general features of the mean observed CO seasonal variations can be reproduced quite well in spite of some underestimations at both sites. In this study, the observed data for the comparison are multi-year averages from 2000 to 2004, while the emissions are estimated for the year 2000 (Streets et al., 2003). The underestimations may be related to the adopted emission inventory, as many studies have showed the trend of increasing pollutant emissions by industrial development and population expansion over East Asia in the recent years (e.g., van Aardenne et al., 1999).

Figure 2 also shows a summer minimum and a winter-spring maximum in the CO seasonal variations. Except the transport processes associated with the Asian monsoon system, this phenomenon should be regarded as the result of photochemical reaction. The major sink of CO in clean air is its reaction with OH, and in summer the production of OH is higher than in other season, thus a CO minimum arises. CO serves

Table 1. Statistical summaries of model results and observations of ozone concentrations (ppbv). $C_{\rm m}$, $C_{\rm ob}$ are the annual average value of modeled and observed quantities, respectively. $\sigma_{\rm m}$, $\sigma_{\rm ob}$ are the averaged standard deviation of the modeled and observed monthly values, respectively. R is the correlation coefficient between observed and modeled quantities.

	Ryori					Yonagunijima				
Year	$C_{\rm m}$	$C_{\rm ob}$	$\sigma_{\rm m}$	$\sigma_{\rm ob}$	R	$C_{\rm m}$	$C_{\rm ob}$	$\sigma_{\rm m}$	$\sigma_{\rm ob}$	R
2000	49.3	39.3	10.2	10.2	0.77	36.7	38.4	11.2	11.0	0.87
2001	48.6	35.5	10.9	8.0	0.61	39.7	39.3	9.7	10.0	0.91
2002	47.8	38.7	11.0	8.8	0.72	40.0	39.1	11.7	12.3	0.81
2003	48.0	41.1	11.4	7.8	0.60	39.2	43.4	10.8	12.3	0.84
2004	53.4	41.0	12.1	8.8	0.69	41.1	42.6	9.4	10.3	0.95

Table 2. Statistical summaries of model results and observations of carbon monoxide (ppbv).

	Ryori					Yonagunijima				
Year	$C_{\rm m}$	$C_{\rm ob}$	$\sigma_{\rm m}$	$\sigma_{\rm ob}$	R	$C_{\rm m}$	$C_{\rm ob}$	$\sigma_{\rm m}$	$\sigma_{\rm ob}$	R
2000	182.7	153.7	38.6	34.1	0.56	165.7	111.8	60.0	34.7	0.53
2001	177.5	153.4	39.4	34.3	0.48	172.7	120.6	62.5	34.6	0.54
2002	188.6	155.9	48.4	38.1	0.31	182.7	155.9	68.2	38.1	0.17
2003	189.7	153.9	42.9	37.9	0.48	195.6	114.7	77.3	34.8	0.58
2004	183.5	175.4	46.7	42.7	0.44	176.8	140.0	61.6	41.2	0.68

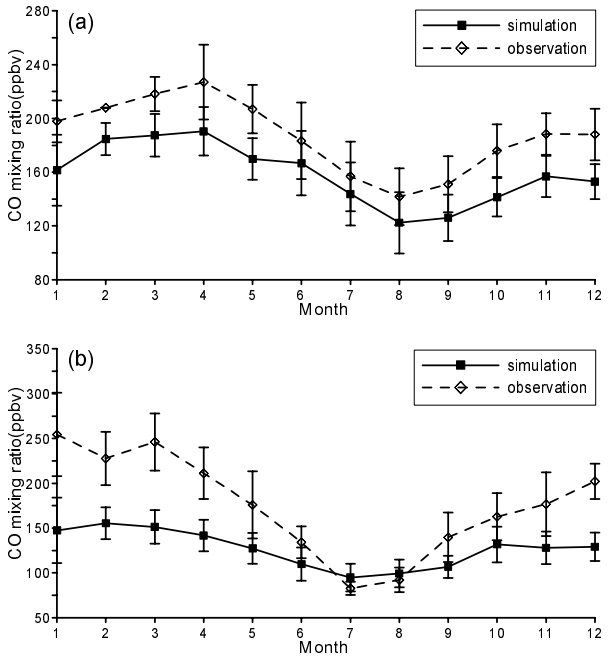

Fig. 2. As Fig. 1 but for CO.

as a tracer of combustion and tropospheric ozone is formed from the combustion byproducts, such as NO_x, hydrocarbons, and CO (e.g., Mauzerall et al., 2000). In air parcels aged from a few days to a week, CO could be a tracer of the photochemically produced ozone. From Figs. 1 and 2 we find that the seasonal variations in surface CO concentration are quite similar to those in ozone at both sites. For ozone and CO, their modeled and observed correlation coefficients are 0.85 and 0.92 at Yonagunijima and 0.38 and 0.83 at Ryori, respectively. The good correlations at these remote sites are thought to be associated with continental outflow, demonstrating the critical role of the rapid transport of carbon monoxide and other ozone precursors from the continental boundary layer.

3.2 *Geographical and seasonal distributions of surface ozone concentrations*

The objective of this study is to analyze typical seasonal variations of tropospheric ozone concentrations over East Asia. The geographical distributions of tropospheric ozone mixing ratios in East Asia in January, April, July, and October of 2001 in the surface layer shown in Fig. 3 are discussed as the year 2001 is a climatologically mean year. To assist in discussing the O_3 behaviors, CO concentration distributions are presented in Fig. 4. These results are presented as monthly averages.

Figure 3 shows that the ozone concentrations have noticeable differences between the four months. Generally the concentrations are higher in the spring and summer and lower in the winter, which agrees well with the seasonal variation of the solar intensity. The seasonal variations are typically strongest over the continental area, reflecting the interactions of solar intensity and photochemical activity.

Figure 3a shows the ozone concentration distributions in the surface layer in wintertime. During this time, the ozone levels are quite low due to the low in-

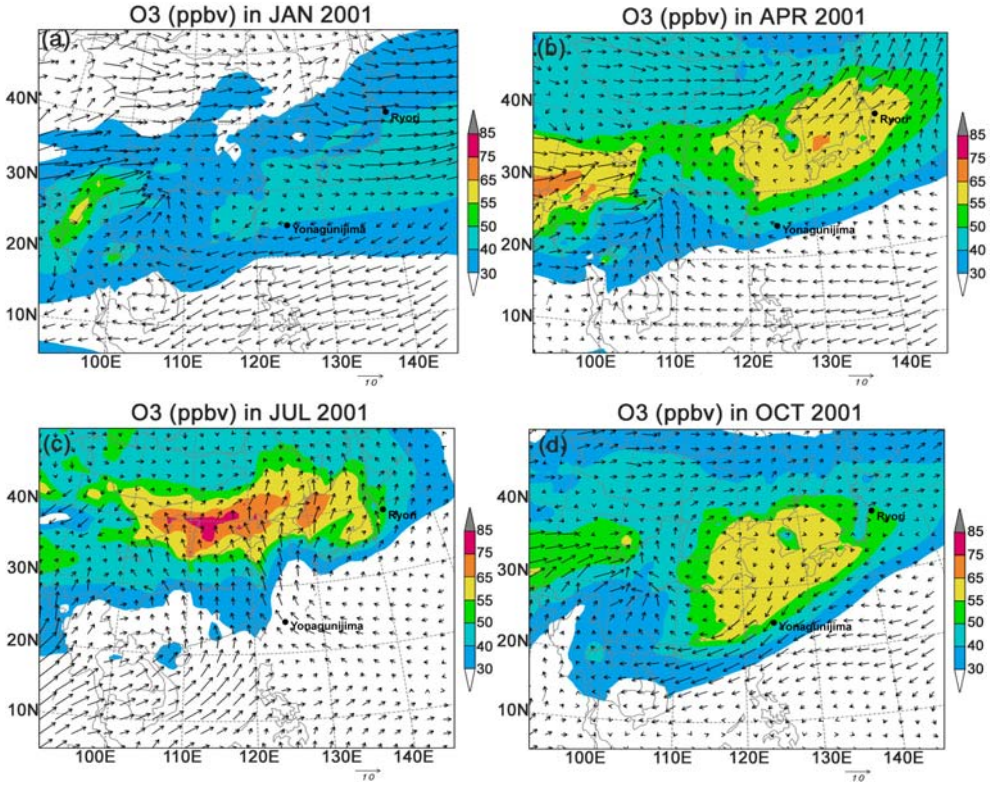

Fig. 3. Horizontal distributions of monthly averaged ozone concentrations (ppbv) and wind vectors in the surface layer in (a) January, (b) April, (c) July, and (d) October of 2001.

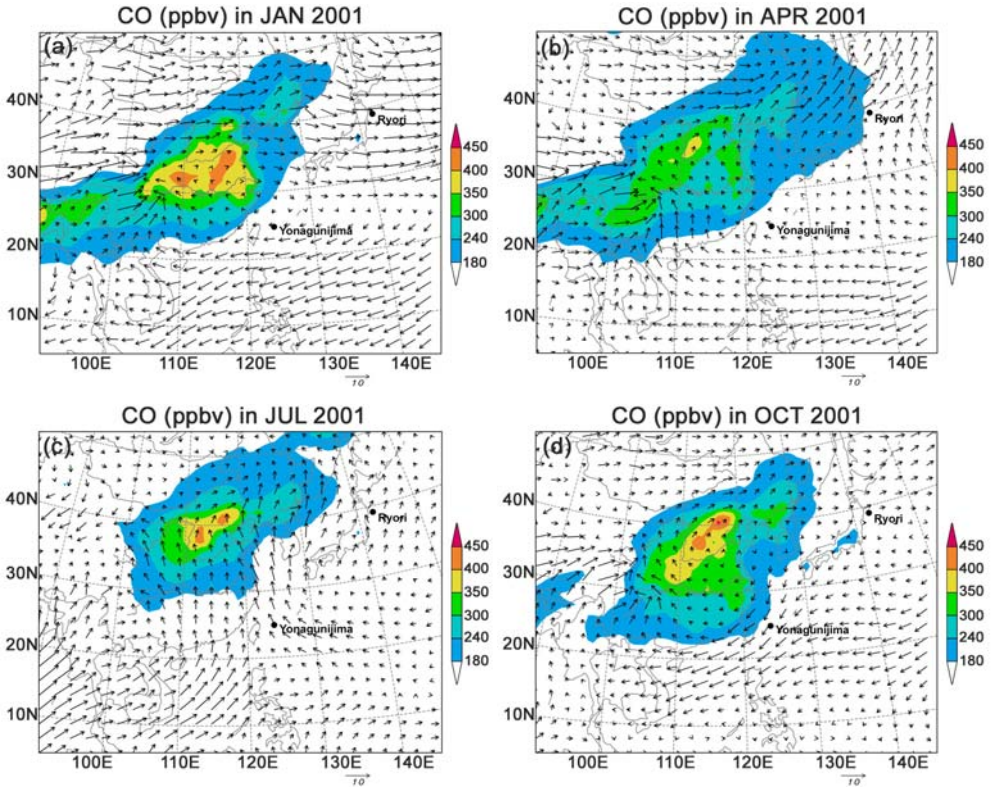

Fig. 4. Same as Fig.3 but for CO.

solation and photochemical activity. The areas with O_3 values higher than 50 ppbv are found over Tibet in association with stratospheric ozone because topography there is over 6500 m above sea level. Relatively high O_3 levels appear in southeastern China and the western Pacific at mid-latitudes. January is under the influence of the winter monsoon in East Asia due to strong pressure gradients between the Siberian High and Okhotsk Low (Ding, 1994). During the peak of the monsoon, there is strong subsidence over the majority of the East Asia continent, and pollution is trapped in the boundary layer. From Fig. 4a we can see that elevated CO concentrations are mainly found over eastern China and its coastal areas with maximum concentrations in an area over central China between the Yangtze River and the Yellow River. This area is characterized by high emissions of CO and other pollutants. The wind flow pattern shown in the figure presents the pollutant transport pathway associated with the continental anticyclones and cold air outbreaks.

Spring is the time that photochemical activity becomes stronger than in winter. The ozone mixing ratio rises during this time. The maximum O_3 value is about 65 ppbv, which occurs in the area covering the Yellow Sea, Korea Peninsula and Japan. By March, the Siberian High weakens and the Pacific high-pressure system is growing. The strong winter monsoon winds decrease, while incursions of warmer and tropical air from the south become frequent. In Fig. 3b, we can see the South China Sea and southern China are dominated by a southwesterly flow coming from the South Asian monsoon region. Clean air brought by this flow dilutes the pollutant, and the ozone mixing ratio stays low in South China, which is mostly under 40 ppbv. Comparing Fig. 3a with Fig. 3b, we can see the isopleth of the 30 ppbv in the south is pushed about 5° to the north in the spring time. But in the northern part (north of 30°N), it is quite different: as shown in Fig. 3b, strong westerlies prevail in this region. The convergence ozone over central and eastern China, where air masses from the north driven by monsoon winds encounter oceanic air masses from the south, plays an important role in the springtime export of pollution from the Asian continent (Zhang et al., 2003).

In July, photochemical reaction is most active, associated with the solar intensity; the highest ozone concentration appears in this season. Meanwhile, the summer monsoon flow has a more southerly component and reaches deep into northern China and even northeastern China (Ding, 1994). Clean maritime air masses dilute the pollutants in the southern part of the whole area (Fig. 3c) and the polluted air masses covering the mainland are pushed further to the north than in spring. We can see that on land, concentration in Yangtze River region is quite different from in the Yellow River region; it reaches the lowest value of the whole year in Yangtze River region (less than 50 ppbv), which represents the south part of China, but reaches the highest value in the whole year in Yellow River region (more than 75 ppbv), which represents the north part of China. In the ocean area, the 30 ppbv isopleth is pushed even deeper into the Yellow sea and south of the Korea Peninsula (about 35°N). That is why the measurements from remote sites in Japan find the summer minimum ozone mixing ratios (e.g., Pochanart et al., 2002). In this season, we can see that ozone changed its maximum area from the northeast part of East Asia (Fig. 3b) to about 40°N in North China (Fig. 3c). Zhu et al. (2004) also find this band of high ozone in their simulation, and explain it as a photochemical product and transport action. Research of Mauzerall et al. (2000) showed that photochemical ozone production is highest in summer in the area north of 20°N. By the above analysis, we also consider the ozone distribution in summer in the East Asia area as the result of photochemistry and summer monsoon transport effects. Figure 4c shows the high CO band in July in nearly the same region as the ozone, which partially proves that the photochemical production is important to the ozone mixing ratios in this area.

In August, the summer monsoon flow weakens, and is completely replaced in October on the China mainland by the winter northeasterly flow, as shown in Fig. 3d. The photochemical reactions also weaken in this season. Ozone concentration falls throughout the whole area. Strong northwesterly continental outflow occurs and the winds sweep pollution northeastward. The maximum level of ozone mixing ratio is about 55 ppbv, in the area of the Yellow Sea and Japan. Figure 3d shows the anticyclonic circulations over central and eastern China. The anticyclonic circulations imply that much of the pollution originating in central and eastern China will flow clockwise out to sea then return to the southwest.

4. Summary

The modeling system RAMS-CMAQ was used to investigate the seasonal variations in tropospheric ozone concentration over East Asia. For the evaluation of the model results, observed surface concentrations of ozone and carbon monoxide at Ryori and Yonaguni-jima were used. Comparison of simulated and observed concentrations over the 5-year period shows that the simulated values are generally in good

agreement with the observations, and their correlation coefficients of the monthly averaged values reach 0.74 and 0.94 for ozone and 0.95 and 0.96 for CO in the two sites, respectively. Observed ozone mixing ratios at Ryori exhibit a clear spring maximum in a clean and remote atmosphere in the mid-latitudes in the Northern Hemisphere. However, at Yonagunijima a minimum in summer and high values in winter-spring were shown, a typical pattern of many remote locations both in the Northern and Southern Hemispheres. The model captured these general features.

Model analysis indicates that monthly averaged surface ozone mixing ratios have noticeable differences among the four seasons. Generally, the concentrations are higher in the spring and summer and lower in the winter, which agrees well with the seasonal variation of the solar intensity. Monsoons over East Asia play an important role in ozone distribution in this area. The winter monsoon carries the pollutants out of the continental region and leads the ozone concentration higher in the remote ocean area than in the mainland in winter and spring. In summer, due to the summer monsoon's diluting and transport effects, the ozone value is low in the south part of East Asia while high in the north part.

Acknowledgements. This study was supported by the National Key Technology R & D program (Grant No. 2007BAC16B01) and the National Basic Research Program (Grant Nos. 2007CB407303 and 2006CB403702).

REFERENCES

Akimoto, H., H. Nakane, and Y. Matsumoto, 1994: The chemistry of oxidant generation: Tropospheric ozone increase in Japan. *The Chemistry of the Atmosphere: Its Impact on Global Change*, J. G. Calvert, Ed., Blackwell Scientific, Cambridge, MA., 261–273.

Byun, D. W., and J. K. S. Ching, Eds., 1999: Science algorithms of the EPA Models-3 community multi-scale air quality (CMAQ) modeling system. EPA/600/R-99/030, NERL, Research Triangle Park, NC.

Carter, W. P. L., 2000: Documentation of the SAPRC-99 Chemical Mechanism for VOC Reactivity Assessment. Final Report to California Air Resources Board, Contract 92–329 and contract 95-308.

Ding, Y., 1994: The summer monsoon in East Asia. Chapter 1, *Monsoons Over China*. Kluwer Academic Publishers, Dordrecht, 1–76.

Holton, J. R., 1990: On the global exchange of mass between the stratosphere and troposphere. *J. Atmos. Sci.*, **47**, 392–395.

Lee, S.-H., H. Akimoto, H. Nakane, S. Kurnosenko, and Y. Kinjo, 1998: Increase of tropospheric ozone at Okinawa, Japan. *Geophys. Res. Lett.*, **25**, 1637–1640.

Lelieveld, J., and F. J. Dentener, 2000: What controls tropospheric ozone? *J. Geophys. Res.*, **105**(D3), 3531–3551.

Mauzerall, D. L., D. Narita, H. Akimoto, L. Horowitz, S. Walters, D. A. Hauglustaine, and G. Brasseur, 2000: Seasonal characteristics of tropospheric ozone production and mixing ratios over East Asia: A global three-dimensional chemical transport model analysis. *J. Geophys. Res.*, **105**(D14), 17895–17910.

Monks, P. S., 2000: A review of the observations and origins of the spring ozone maximum. *Atmos. Environ.*, **34**, 3534–3561.

Olivier J., J. Peters, C. Granier, G. Petron, J. F. Muller, and S. Wallens, 2003: Present and future surface emissions of atmospheric compounds. POET report No. 2, EU project EVK2-1999-00011.

Oltmans, S. J., and Coauthors, 1998: Trends of ozone in the troposphere. *Geophys. Res. Lett.*, **25**, 139–142.

Pielke, R. A., and Coauthors, 1992: A comprehensive meteorological modeling system-RAMS. *Meteorology and Atmospheric Physics*, **49**, 69–91.

Pochanart, P., H. Akimoto, Y. Kinjo, and H. Tanimoto, 2002: Surface ozone at four remote island sites and the preliminary assessment of the exceedances of its critical level in Japan. *Atmos. Environ.*, **36**, 4235–4250.

Streets, D. G., and Coauthors, 2003: An inventory of gaseous and primary aerosol emissions in Asia in the year 2000. *J. Geophys. Res.*, **108**, D21.8809.

Tang, J., and Coauthors, 1995: Surface ozone measurement at China GAW baseline observatory. *Conference on the Measurement and Assessment of Atmospheric Composition Change*, World Meteorol. Organ., Int. Global Atmos. Chem., Beijing.

van Aardenne, A. J., G. R. Carmichael, H. Levy II, D. G. Streets, and L. Hordijk, 1999: Anthropogenic NO_x emissions in Asia in the period 1990–2020. *Atmos. Environ.*, **33**, 633–646.

Zhang, M., I. Uno, S. Sugata, Z. F. Wang, D. Byun, and H. Akimoto, 2002: Numerical study of boundary layer ozone transport and photochemical production in east Asia in the wintertime. *Geophys. Res. Lett.*, **29**(11), 1545, doi: 10.1029/2001GL014368.

Zhang, M., Y. F. Xu, I. Uno, and H. Akimoto, 2004: A numerical study of tropospheric ozone in the springtime in East Asia. *Adv. Atmos. Sci.*, **21**, 163–170.

Zhang, M., and Coauthors, 2003: Large-scale structure of trace gas and aerosol distributions over the western Pacific Ocean during TRACE-P. *J. Geophys. Res.*, **108**(D21), 8820, doi: 10.1029/2002JD002946.

Zhu, B., H. Akimoto, Z. Wang, K. Sudo, J. Tang, and I. Uno, 2004: Why does surface ozone peak in summertime at Waliguan? *Geophys. Res. Lett.*, **31**, L17104, doi: 10.1029/2004GL020609.